sustainability

Article

Determination of the Influence of the Disturbance Caused by Traversing Cross-Type Deep Foundation Pit Excavations

Shuhong Wang [1], Bo Yang [1,*], Furui Dong [1], Marinichev Maxim [2] and Ze Zhang [1]

1 School of Resources & Civil Engineering, Northeastern University, Shenyang 110819, China
2 Kuban State Agrarian University (KubSAU), 13 Kalinina Str., 350044 Krasnodar, Russia
* Correspondence: 2071098@stu.neu.edu.cn

Abstract: Accurately recognizing the influence of excavation disturbance on the traversing cross-type deep foundation pit of the subway, determining the active range of the disturbance, and reasonably arranging the structure within its range can effectively ensure the safety of the project and save resources to achieve the goal of sustainable development. A three-dimensional model was established using the soil small strain hardening model to examine the subway deep foundation pit project in the CBD (central business district) core area of Fuzhou Coastal New City, where the soil is mainly soft soil with high natural water content, high compressibility, and weak permeability. The model was verified against the theoretical solution of Melan, and the deformation characteristics of the cross-asymmetric foundation pit excavation were analyzed. The results show that, due to repeated disturbance from excavation and unloading between the foundation pits, the soil arching effect, and changes in the boundary conditions, the structure at the intersection and the surrounding soil interact. The horizontal displacement of the retaining structure and the surrounding surface settlement are quite different from those observed from a single foundation pit excavation. For instance, the maximum horizontal displacement of profile 1-3 in Zone I decreases by 26.1%, while the maximum horizontal displacement of profile 1-1 in Zone II increases by 20.4%, and the maximum surface settlement around the profiles also has similar characteristics. The disturbance on the retaining structure and soil in different areas at the intersection can be divided into positive and negative effects. The active range of the "disturbance influence zone" is determined: the foundation pit of Metro Line 6 is 3.5 He and the foundation pit of Metro Line F1 is 3.0 He. Finally, the influence of changes in the groundwater level on the active range of the "disturbance influence zone" is discussed.

Keywords: traversing cross-type deep foundation pit; the hardening strain model with small strain; cross position; disturbance influence; active range

Citation: Wang, S.; Yang, B.; Dong, F.; Maxim, M.; Zhang, Z. Determination of the Influence of the Disturbance Caused by Traversing Cross-Type Deep Foundation Pit Excavations. *Sustainability* **2023**, *15*, 1130. https://doi.org/10.3390/su15021130

Academic Editor: Gianluca Mazzucco

Received: 4 November 2022
Revised: 29 December 2022
Accepted: 4 January 2023
Published: 6 January 2023

1. Introduction

Rail transit in cities has expanded rapidly along with the necessary urban infrastructure, while the available land in central urban areas has gradually reduced. Regional deep foundation pits to accommodate the various urban infrastructures have appeared in great numbers. Currently, a large number of foundation pits are constructed at the same time or to traverse existing foundation pits. In practical engineering, the mutual influence of adjacent foundation pit construction significantly increases the engineering safety risks [1].

Currently, the impact of foundation pit construction on the environment mainly focuses on the deformation of the retaining structure and surrounding soil. Through on-site real-time monitoring and finite element numerical simulation analysis, the expected deformation of the structure and the adjacent soil during excavation of the foundation pit can be reasonably well predicted [2,3]. Because the adjacent foundation pit excavation process is affected not only by the foundation pit itself but also by the adjacent foundation pit construction [4,5], the stresses and deformations of the adjacent foundation pit become more complex, attracting extensive attention from scholars.

In theoretical research, Fengwen Lai et al. [6] established a universal solution method of finite active earth pressure based on the sliding-wedge method and the finite difference theory. According to the limit equilibrium theory, Xiaoyu Chen et al. [7] came up with an expression for the critical spacing of interaction between adjacent foundation pits. Using long-term field displacement monitoring data, Song et al. [8] analyzed the problem and put forward the law that the impact of a foundation pit excavation on the surrounding environment decreases with an increase in the distance from the excavation area. Zeng et al. [9] analyzed the deformation characteristics of adjacent foundation pit retaining structures and adjacent soil using field measurements. Chen et al. [10] observed the deformation characteristics of deep foundation pit groups and the interaction between adjacent foundation pits through a monitoring system. In terms of numerical simulation, Lianxiang Li et al. [11] analyzed the deformation characteristics of a foundation pit excavated parallel to an existing station using a three-dimensional finite element analysis and proposed corrective control measures. Hou et al. [12] examined the interaction between adjacent foundation pit excavations employing the finite element method and proposed a theoretical method of sub-regional excavation of the foundation pit. Although many scholars have carried out research on the excavation of adjacent foundation pits, the influence and scope of disturbance on the excavation of the cross-type asymmetric foundation pits is still unclear. Therefore, it is necessary to carry out further research.

This paper is organized as follows. Firstly, the parameters of the small strain hardening model of soil are determined, a three-dimensional finite element model of the foundation pit is established, and the deformation characteristics of the structure and surrounding soil in the intersecting area are analyzed. Then, according to the disturbance influence of different effects in this domain, the positive and negative are divided and the active range of the "disturbance influence zone" is determined. Finally, the influence of groundwater level changes on the "disturbance influence zone" is discussed. This study provides a reference for the construction, design, and deformation control for deep foundation pits that traverse one another.

2. Traversing Cross-Type Deep Foundation Pits and Limitations of Deformation Control

2.1. Traversing Cross-Type Deep Foundation Pit

From a geometric point of view, a traversing cross-type deep foundation pit is composed of the cross sections of each different pit spacing of adjacent parallel foundation pits, as shown in Figure 1. The interaction between the structure and the surrounding soil during the excavation process is not a simple superposition relationship, which inevitably poses new problems for the project.

2.2. Limitations of Cross Position Deformation Control

At present, the intersection position is the critical point in the deformation control of a cross-type deep foundation pit. During the project construction, multiple monitoring points are often arranged at this position to monitor the deformation of the foundation pit in real time. However, due to the failure to accurately analyze the influence of the disturbance generated by the excavation, deformation control of the foundation pit is not properly controlled or is too conservative, increasing the safety risks and economic losses to the project. Therefore, it is necessary to accurately determine the "disturbance influence zone" for cross-type deep foundation pit engineering.

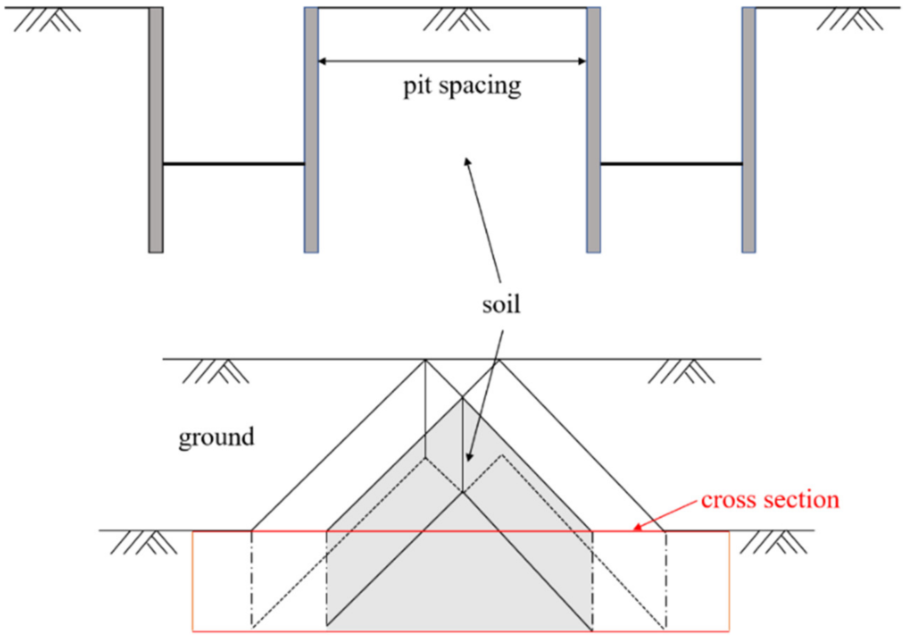

Figure 1. Schematic diagram of traversing cross-type foundation pit.

3. FE Analysis

3.1. Field Study

The supporting project is located in the CBD core area of Fuzhou Coastal New City, with a total construction area of about 250,000 square meters. It is a vast underground TOD (transit-oriented development) complex. The east–west span of the project is 570 m, and the north–south span is 370 m. The underground structure is divided into three major parts: the plot foundation pit, the subway foundation pit, and the ramp foundation pit. The subway foundation pit is comprised of the east end shaft, the standard section of Line F1, Line 6, and the west end shaft. The general layout of the foundation pit is shown in Figure 2.

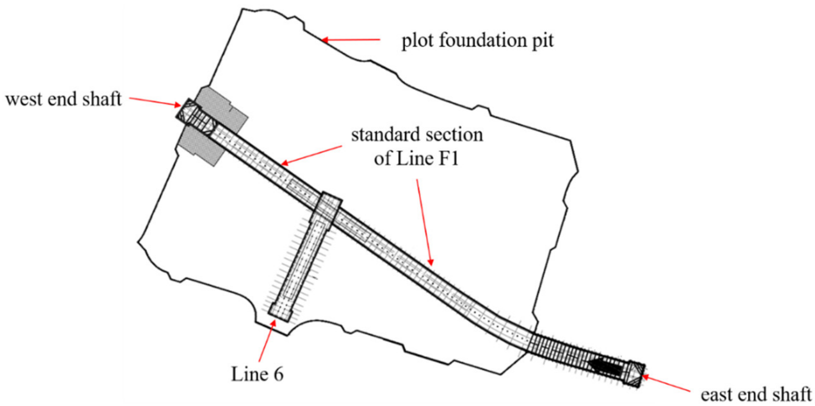

Figure 2. General layout of foundation pit.

According to the survey report, the soil stratum of the project is mainly composed of miscellaneous fill, silty clay, muddy soil, sandy soil, and a strongly weathered granite. The groundwater level is about 2.5 m below the ground during the foundation pit excavation.

3.2. Soil Constitutive Model and Parameter Selection

When the excavation depth of the foundation pit exceeds a specific range, the depth effect will be generated. The traditional Mohr–Coulomb model cannot accurately reflect the deformation of the deep foundation pit [13]. The small strain hardening model of soil (HSS) can be considered for the stiffness characteristics, loading and unloading effects, hardening characteristics, and the dependence of stiffness on the stress history and path of soil under small strain conditions. Therefore, it is an appropriate choice for simulating soil excavation problems [14].

All small strain hardening model parameters of the soil can be determined from laboratory tests [15]. Some parameter values used in this paper were obtained from the geological exploration report, while others were obtained from the research results of reference [16]. The specific parameters are shown in Table 1.

Table 1. Physical and mechanical parameters of soils in the HSS model.

Soil Layer	c'/KPa	φ'/(°)	E_{oed}^{ref}/MPa	E_{50}^{ref}/MPa	E_{ur}^{ref}/MPa	G_0^{ref}/MPa	$\gamma_{0.7}$/10^{-4}	m	K_0	R_f
Silty clay	27	14	6.7	6.6	32.0	97.0	2.7	0.80	0.76	0.9
Mucky soil①	20	15	2.5	3.7	20.0	60.0	2.6	0.70	0.74	0.9
Sand	6	30	22.0	22.0	66.0	200.0	2.5	0.65	0.50	0.9
Mucky soil②	21	25	2.6	3.9	21.0	60.5	2.5	0.70	0.58	0.9
Granite	30	36	3.6	3.6	22.5	67.5	3.0	0.65	0.41	0.9

Note: c', φ', and R_f are strength related parameters; E_{oed}^{ref}, E_{50}^{ref}, E_{ur}^{ref}, m, and K_0 are stiffness related parameters; G_0^{ref} and $\gamma_{0.7}$ are small strain parameters. The parameters can be obtained one by one through the methods provided in reference [16].

3.3. Assumptions and Establishment of the Finite Element Model

To facilitate the implementation of the simulation software, as well as considering the complexity of the project, and with some relevant references [7,11], the following assumptions are made:

(1) The interface of each soil layer on the site is assumed to be horizontal, and the thickness is taken as the average value.
(2) The physical and mechanical properties of the cast-in-place pile and diaphragm wall remain unchanged along the depth, and the friction contact coefficient with the surrounding soil layer is not affected by depth.
(3) Excluding the influence of some interlayer soils, the soil quality is uniform within the same depth range; any inhomogeneity in the actual soil layer is not considered.
(4) This paper focuses on the deformation characteristics of the intersection of the subway deep foundation pit. The influence of the plot foundation pit is not considered.
(5) In view of the construction process for the foundation pit, the numerical simulation is based on the one-time layer-by-layer excavation without considering the impact of segmented and block excavation.

The influence of size effects on the model needs to be eliminated (generally, the affected width of foundation pit excavation is 3–4 times the pit depth, and the affected depth is 2–3 times the pit depth). In addition, considering the construction of the east end shaft of the project, the dimension of the three-dimensional numerical model of this cross-type deep foundation pit can be 500 m × 700 m × 60 m.

In the three-dimensional model, a plate element is used to simulate the wall panel structure, an embedded pile element is used to simulate the erect column pile, and a beam element is used to simulate the concrete support, steel support, and steel connecting rod, etc. The pile wall in the standard section of Metro Line 6 can be converted into an underground diaphragm wall according to Equation (1).

$$\frac{1}{12}(D+c)T^3 = \frac{1}{64}\pi D^4 \tag{1}$$

where D is the diameter of the cast-in-place pile. C is the net spacing between the rows of piles; when the piles are in the horizontal bite state, C is taken as a negative value. T is the thickness of the underground diaphragm wall.

Then, 900@1200 (the diameter of cast-in-place piles is 900 mm and the spacing is 1200 mm) row piles are converted into the underground diaphragm walls with a thickness of 685 mm.

Since the structure at the intersection of the foundation pit in this project needs to be reinforced before excavation, the capacity of its support system will be enhanced; when attributes are assigned to the structure, appropriate corrections should be made to ensure the accuracy of the calculation results. The structural parameters in the model are detailed in Tables 2 and 3.

Table 2. Internal support and column pile parameters.

Type \ Parameter	Elastic Modulus $E/(\mathrm{GPa})$	Cross Sectional Area $A/(\mathrm{m}^2)$
Concrete purlin	30.0	0.96
Steel purlin	200.0	0.21
Concrete support	31.5	0.64
Steel support	200.0	0.03
Concrete connecting rod	31.5	0.36
Steel connecting rod	200.0	4×10^{-5}
Erect column pile	30.0	0.50

Table 3. Parameters of retaining structure.

Type \ Parameter	Thickness h/m	Gravity Density $\gamma/\mathrm{kN{\cdot}m^{-3}}$	Elastic Modulus E/GPa	Poisson Ratio ν
Diaphragm wall of west end shaft	1.0	26	32.5	0.2
Row piles of the standard section of Metro Line F1	0.685	24	31.5	0.2
Diaphragm wall of east end shaft	1.0	27	32.5	0.2
Diaphragm wall of Metro Line 6	0.8	25	32.5	0.2

The first-floor support of the foundation pit of the standard section of Metro Line F1 employs concrete supports with an average spacing of about 8 m; the second and third floor supports use steel supports with an average spacing of about 4.5 m. The first and second floors of the foundation pit of Metro Line 6 are supported by concrete, with an average spacing of about 6 m; the third and fourth floors are supported by steel, with an average spacing of about 2 m. The cross-sectional view of the support arrangements is shown in Figure 3.

3.4. Simulation of Construction Conditions

According to the construction scheme of the project, the construction of the west end shaft will be carried out first, and then the cross construction will be carried out synchronously from the intersection of Metro Line F1 and Line 6 on both sides. A method of supporting while digging will be adopted. Finally, the construction of the east end shaft will be carried out. This paper mainly studies the deformation characteristics of the intersection of Metro Line F1 and Line 6 and performs local refinement of the structure of the intersection of the foundation pit to achieve the targeted research. The specific construction process is shown in Figure 4.

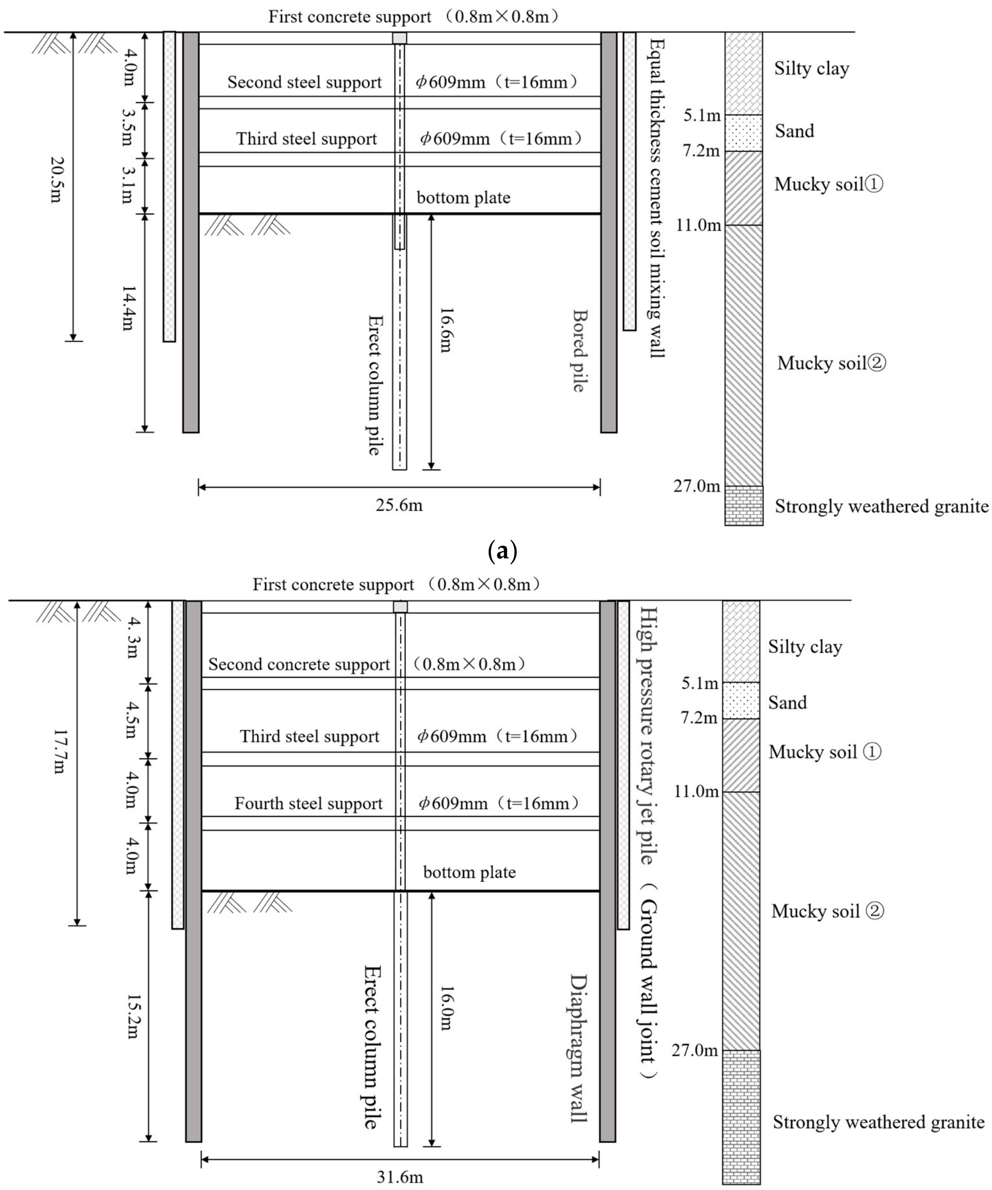

(**a**)

(**b**)

Figure 3. Profile of support layout. (**a**) Metro Line F1; (**b**) Metro Line 6.

Studies have shown that mesh size and quality significantly affect the accuracy of numerical analyses [17]. The runtime of the analysis also depends on the mesh size, quality, and model size. When the calculation time and mesh quality are appropriate, it is then necessary to establish multiple groups of models for scientific research (combining global and local modeling) to better carry out targeted research on the intersection problem studied in this paper. The mesh division adopts the method of overall medium and structural densification and optimization, as shown in Figure 5. The boundary condition of the model adopts the default boundary constraint in PLAXIS 3D; that is, the lateral side adopts the horizontal constraint, the bottom adopts the fixed constraint, and the upper surface is free.

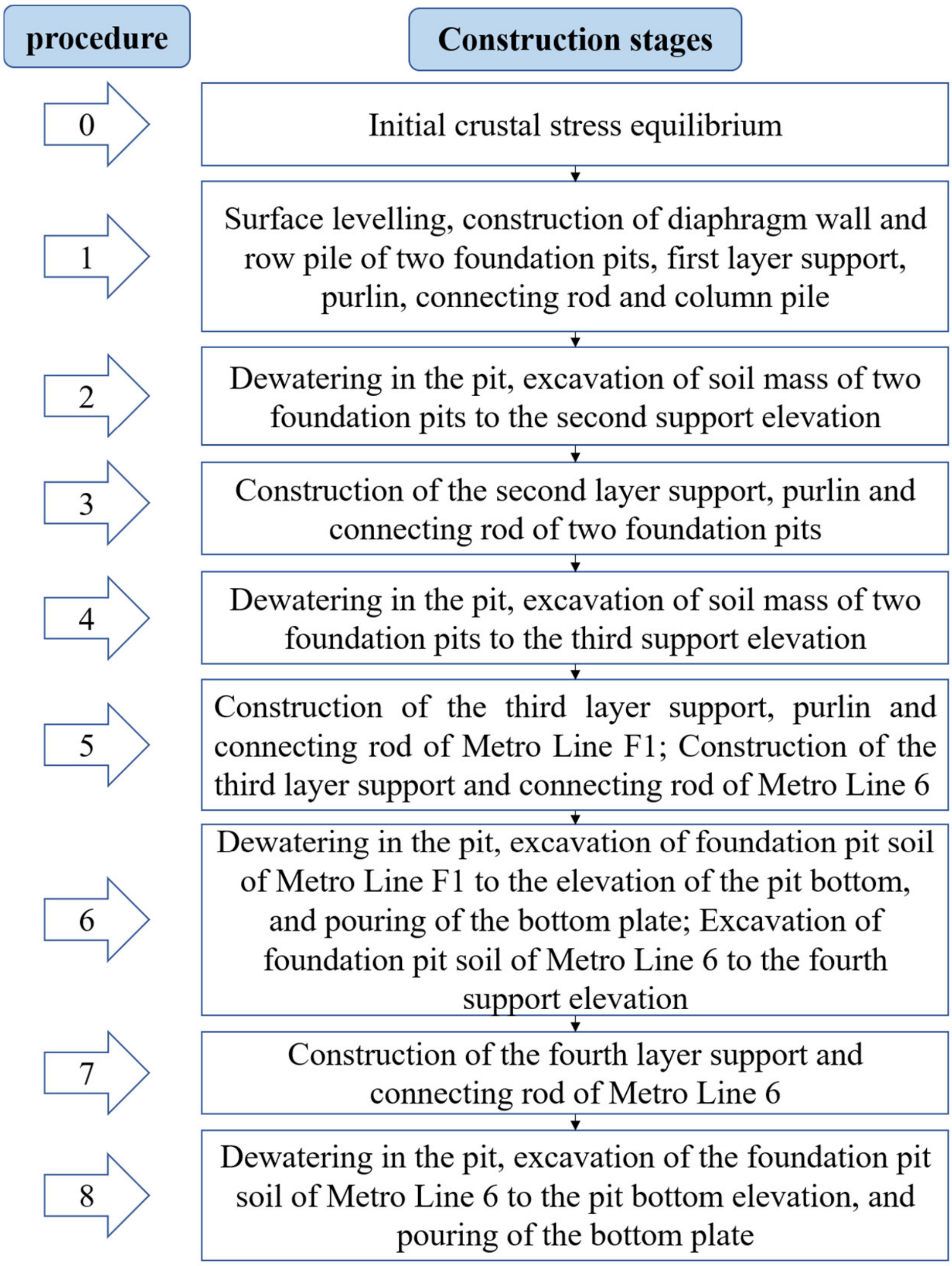

Figure 4. Construction and excavation procedures of Metro Lines F1 and 6.

3.5. Verification of the Rationale of the Computational Model

3.5.1. The Theoretical Analysis of Foundation Pit Excavation Stress Based on Melan

The numerical solution of the stress at any point in a foundation pit excavation can be solved by the theoretical formula proposed by Melan [18].

In the elastic semi-infinite space, there is a strip load of width b along the negative x direction, as shown in Figure 6. By integrating the Melan solution, the stress solution at any point in this region is:

$$\begin{aligned}\sigma_X = \frac{q}{2\pi(1-v)}\Big[&\frac{1}{2}\arctan\frac{h-z}{x} + \frac{x(h-z)}{2r_1} - \\ &\frac{1}{2}\arctan\frac{h+z}{x} - \frac{2xzh(h+z)}{r_2^4} - \frac{x(5h+z)}{2r_2^2} \\ &+\frac{1-2v}{2}\left(\arctan\frac{h-z}{x} + 3\arctan\frac{h+z}{x} + \frac{2xz}{r_2^2}\right)\Big]\Bigg|_{h=h_1}^{h=h_2}\end{aligned} \tag{2}$$

$$\sigma_z = \frac{q}{2\pi(1-v)}\left[\frac{1}{2}\arctan\frac{h-z}{x} - \frac{x(h-z)}{2r_1^2} - \frac{1}{2}\arctan\frac{h+z}{x} + \frac{2xhz(h+z)}{r_2^4} + \frac{x(h+z)}{2r_2^2} - \frac{1-2v}{2}\left(\arctan\frac{h-z}{x} - \arctan\frac{h+z}{x} + \frac{2xz}{r_2^2}\right)\right]\Bigg|\begin{matrix} h = h_2 \\ h = h_1 \end{matrix} \tag{3}$$

$$r_1^2 = x^2 + (z-h)^2, r_2^2 = x^2 + (z+h)^2 \tag{4}$$

where q is the linear load; v is the Poisson's ratio; h is the depth of action of the linear load; x is the horizontal coordinate of a point in the semi-infinite space; and z is the ordinate of a point in the semi-infinite space.

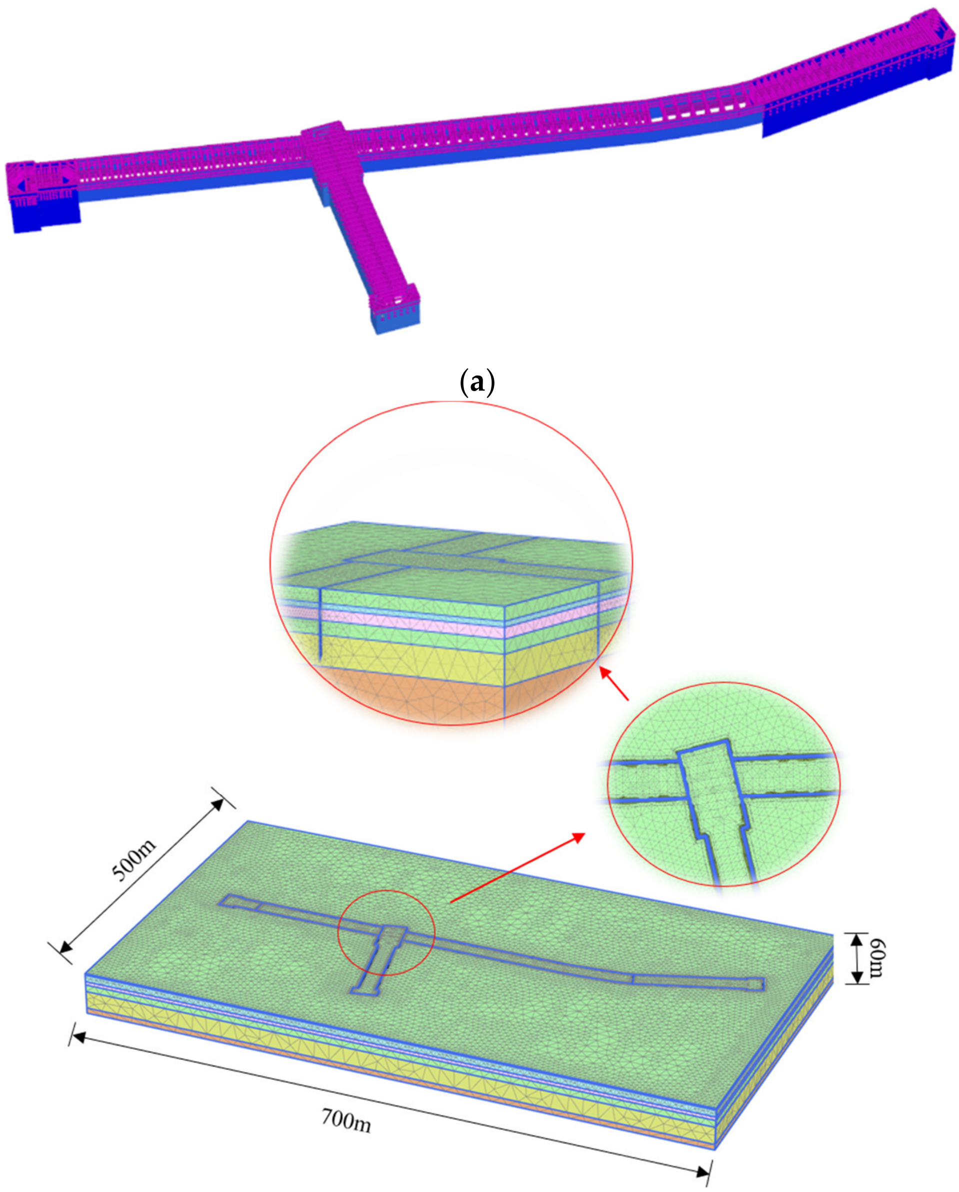

(**a**)

(**b**)

Figure 5. Structural model and mesh division. (**a**) Geometric model; (**b**) mesh division.

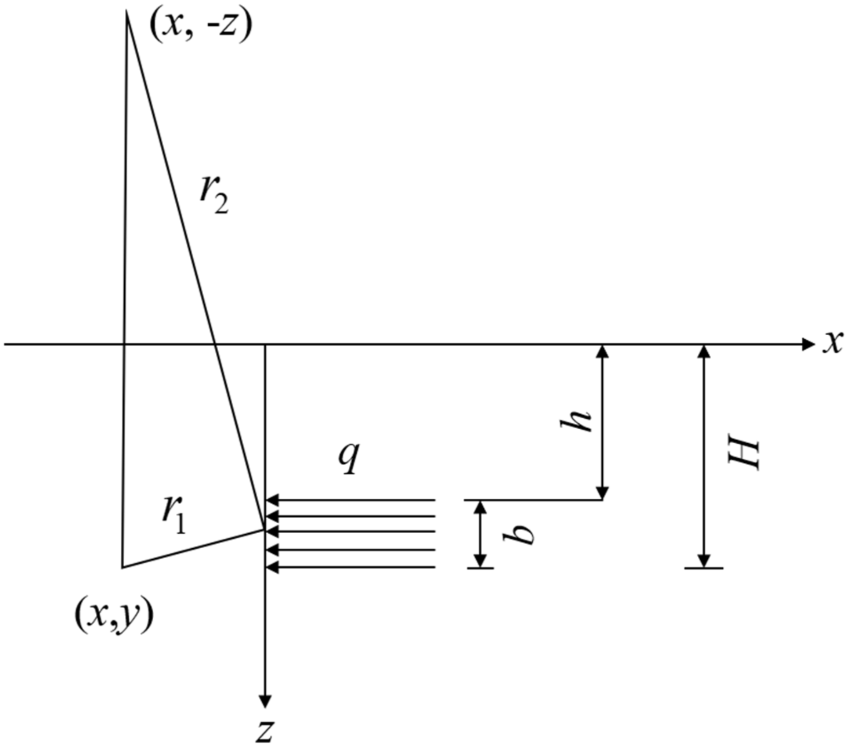

Figure 6. Melan's solution under strip load.

3.5.2. Calculation and Model Verification of the Deformation of the Foundation Pit

The excavation and unloading of the foundation pit will lead to the redistribution of in situ stress, resulting in extensive changes in the physical and mechanical properties of the soil in the foundation pit [19]. In this section, the method proposed in Reference [20] is used to calculate the horizontal displacement of the wall and the ground settlement behind the wall caused by the excavation of the foundation pit based on the Melan solution and the foundation pit deformation calculation method that considers the stress path. The rationale for the model is verified by comparing it with the simulation calculation results.

When calculating the stress and displacement of the corresponding points in the foundation pit structure and the surrounding soil, it is considered to be an isotropic plane strain problem [18], with the following physical and geometric Equations (5) and (6), respectively.

$$\begin{cases} \varepsilon_x = \frac{1-v^2}{E}\left(\sigma_x - \frac{v}{1-v}\sigma_z\right) \\ \varepsilon_x = \frac{\partial u_x}{\partial x} \end{cases} \tag{5}$$

$$\begin{cases} \varepsilon_z = \frac{1-v^2}{E}\left(\sigma_z - \frac{v}{1-v}\sigma_x\right) \\ \varepsilon_z = \frac{\partial u_z}{\partial z} \end{cases} \tag{6}$$

where E is the Elastic Modulus; v is the Poisson ratio of the material. Both are elastic constants [20].

Figures 7 and 8 show the comparison curves of the theoretical, empirical [21], and numerical simulation calculations for the horizontal displacement of the foundation pit retaining structure and the surrounding surface settlement, respectively. The results show that the deformation characteristics obtained from the calculation model are essentially consistent with the results of the theoretical solutions and empirical values, and the average absolute error is less than 10%, which verifies the rationale for the foundation pit calculation model.

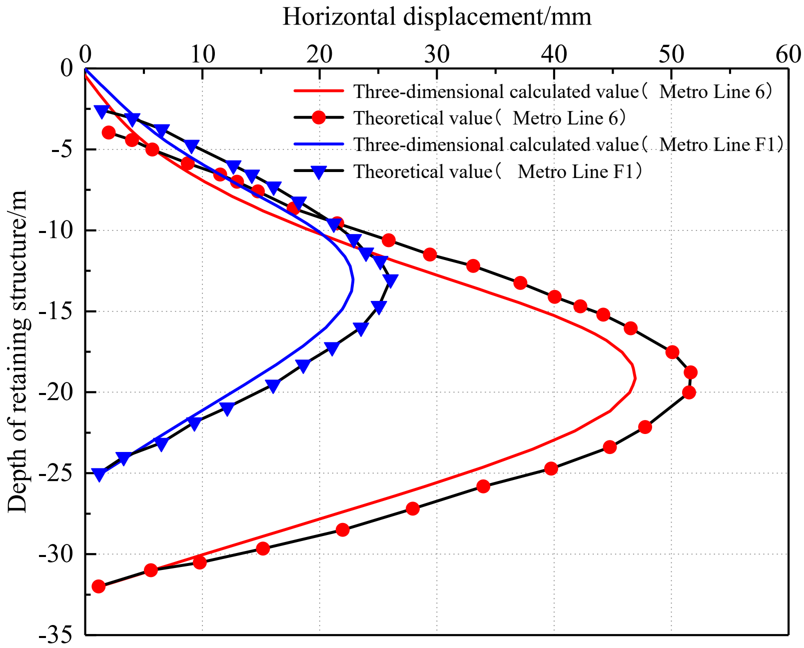

Figure 7. Horizontal displacement of the retaining structure.

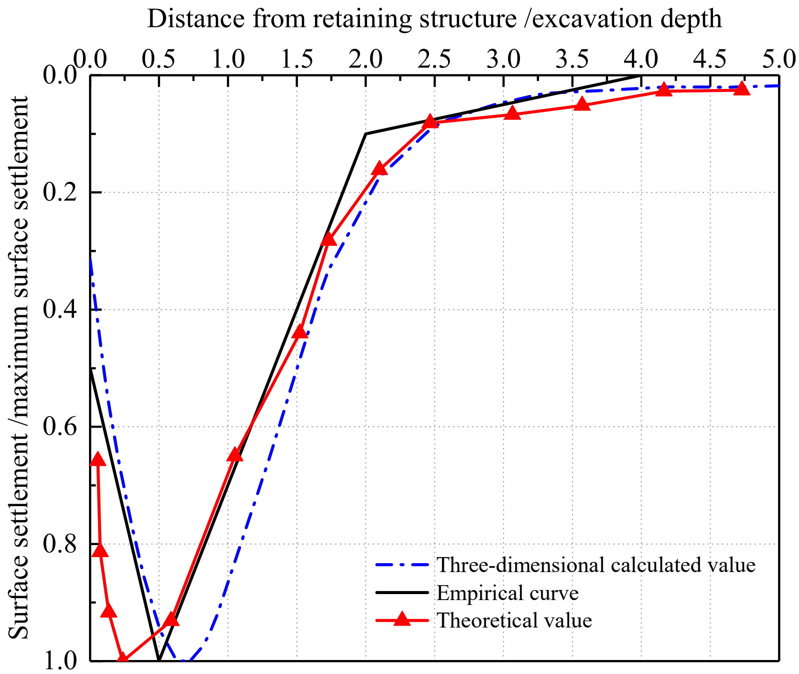

Figure 8. Ground surface settlement.

4. Analysis of Numerical Results

4.1. Horizontal Displacement of Retaining Structure

The horizontal displacement of the retaining structure is an important index to measure the safety of the foundation pit. Based on the analysis of the intersection of Metro Line F1 and Line 6, it is found that there are several places with obvious large deformations in the retaining structure of Metro Line 6 (deep foundation pit). According to the layout of on-site monitoring points, the foundation pit profiles 2-1 and 2-2 of the standard section of Metro Line F1 at the intersection and 1-1, 1-2, 1-3, and 1-4 of the foundation pit profiles of Metro Line 6 have been identified as typical profiles. The intersection area is divided into Zone I and Zone II, as shown in Figure 9.

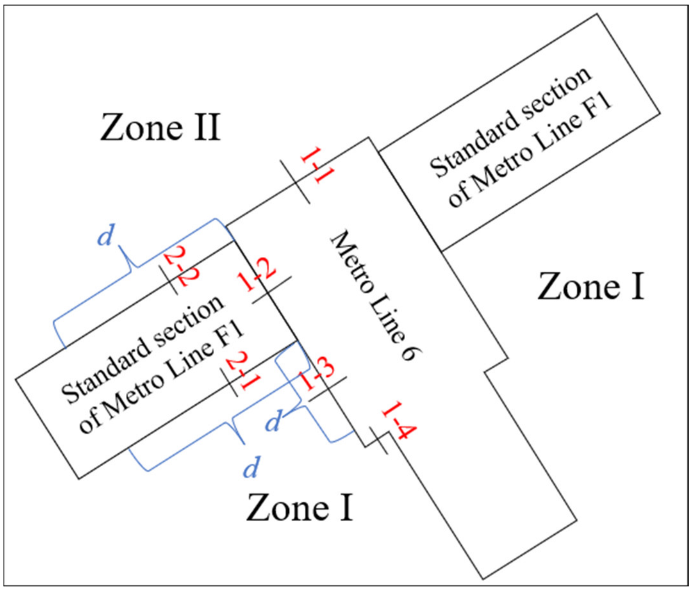

Figure 9. Schematic diagram of typical profile at the cross position.

To study the deformation characteristics of the foundation pit retaining structure of Metro Line 6, typical profiles were selected for this research. Figure 10 shows the horizontal displacement curve of the retaining structure of the typical profile of the foundation pit of Metro Line 6 during simultaneous excavation of the adjacent foundation pits.

It can be seen from Figure 10 that the maximum horizontal displacement of the retaining structure at the 1-1 profile of the foundation pit of Metro Line 6 is 57.9 mm, which is the maximum value recorded at the intersection. The maximum horizontal displacement of the retaining structure of the 1-4 profile is 17.8 mm, which is the minimum value in this typical section of Line 6 (the maximum horizontal displacement of the structure). However, since there is no support on the wall top, there is a large horizontal displacement. During the construction process, deformation control and real-time monitoring should be carried out to ensure the safety and stability of the foundation pit. From the deformation information on deep foundation pits summarized in the literature [22] and the horizontal displacement of the foundation pit in this project, it can be seen that the deformation of the retaining structure at the intersection of the adjacent foundation pits has different deformation characteristics to those observed in individual foundation pit excavations, as shown in Figure 11; the maximum horizontal displacement has decreased.

Profile 1-2 belongs to the common wall part of Metro Line F1 and Line 6. It can be seen from Figure 10b that the horizontal displacement of its retaining structure is mainly caused by the excavation of the fourth layer of soil in its own foundation pit, with a maximum deformation of 20.2 mm. However, in the synchronous excavation with the standard section of Metro Line F1, the deformation is relatively small, and the maximum value is only 8.6 mm.

Profiles 2-1 and 2-2 are two symmetrical profiles of the foundation pit of the standard section of Metro Line F1. When a separate foundation pit is excavated, the horizontal displacement of the retaining structure of the symmetrical section is basically the same, but in this cross-type deep foundation pit, the maximum horizontal displacement of the symmetrical section differs by 2.6 mm, as shown in Figure 12. After excavation of the fourth floor of Metro Line 6, the horizontal displacement of the retaining structure of profile 2-1 in Zone I has changed significantly, with the maximum horizontal displacement increasing by 1.2 mm, while the maximum horizontal displacement of profile 2-2 in Zone II only increased by 0.26 mm. The difference in these deformation characteristics, to some extent, indicates that the excavation of cross-type adjacent foundation pits has different effects on the retaining structure.

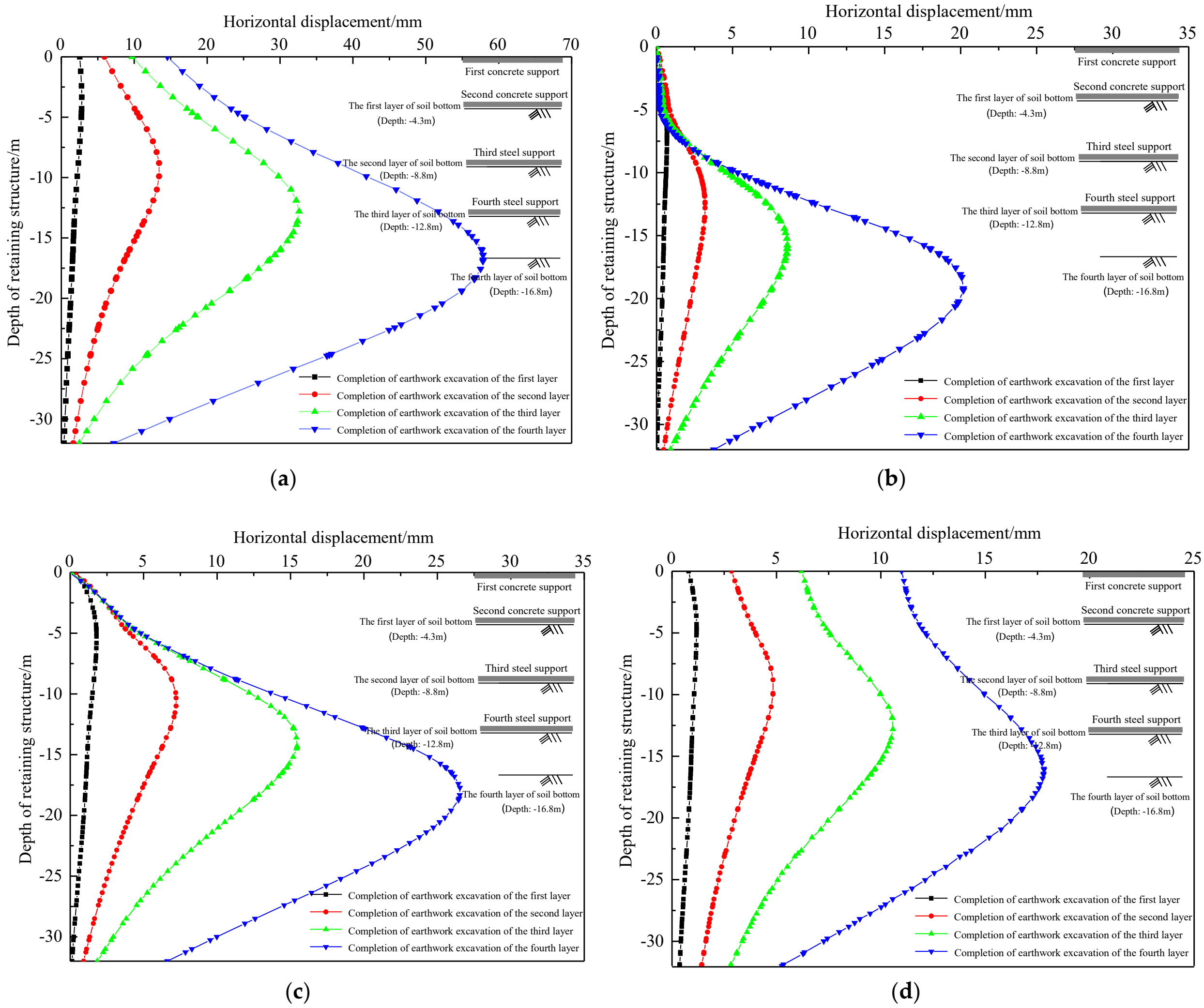

Figure 10. Horizontal displacement of typical profile of the foundation pit of Metro Line 6. (**a**) 1-1 profile; (**b**) 1-2 profile; (**c**) 1-3 profile; (**d**) 1-4 profile.

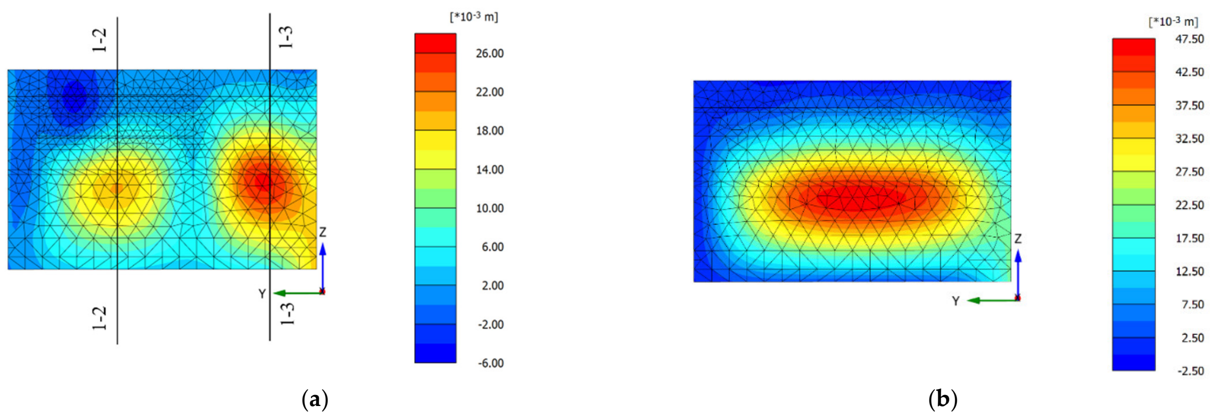

Figure 11. Horizontal displacement of part of the retaining structure of the foundation pit of Metro Line 6. (**a**) Simultaneous excavation; (**b**) individual excavation (The * in the figure represents multiplication sign).

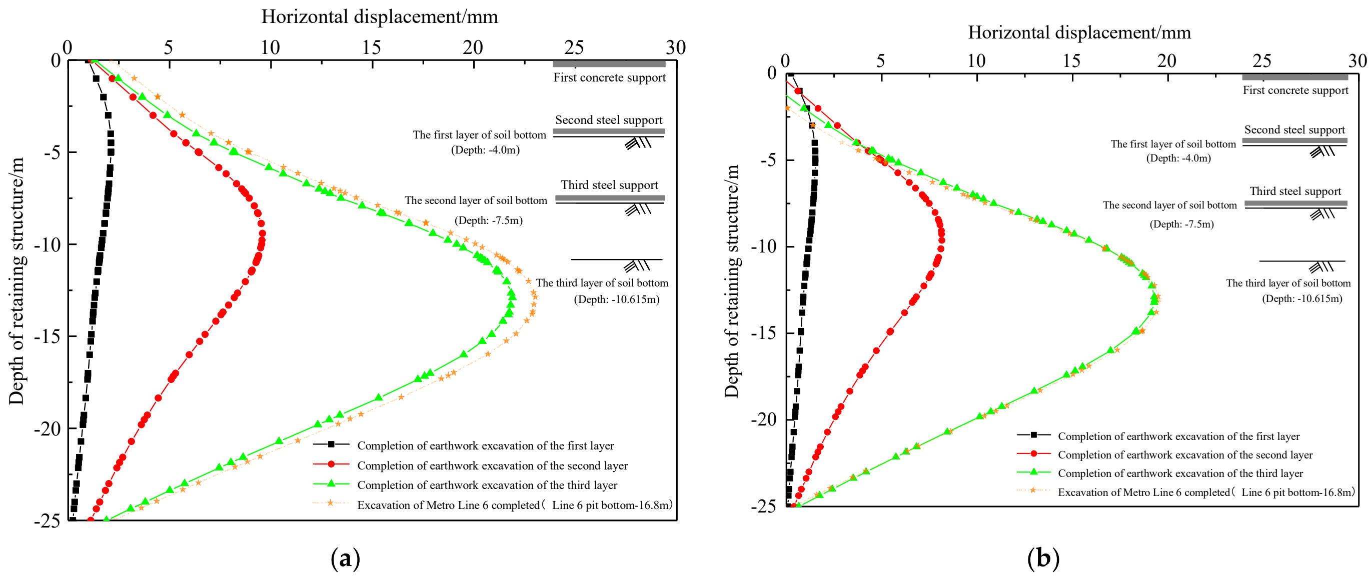

Figure 12. Horizontal displacement of typical profile of foundation pit in a standard section of Metro Line F1. (**a**) 2-1 profile; (**b**) 2-2 profile.

4.2. Analysis of Surface Settlement

Figure 13 shows the nephogram of the cumulative vertical displacement of the soil mass in the final stage of the foundation pit excavation. The general trend of ground settlement around the foundation pit can be seen in the figure. The soil mass near the typical profile of the retaining structure in Zone I and Zone II was selected for surface settlement analysis. The characteristic curve of surface deformation is shown in Figure 14.

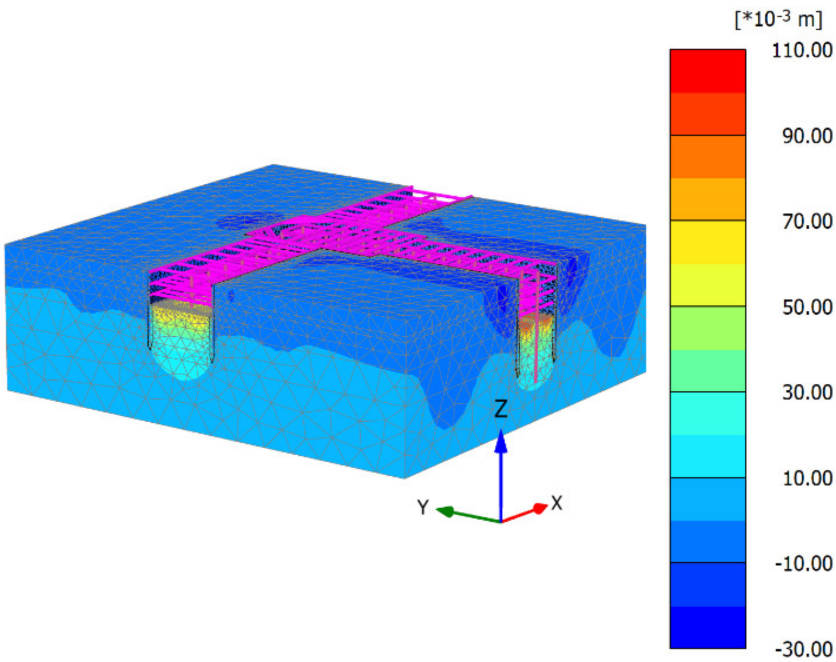

Figure 13. Vertical displacement of the soil (The * in the figure represents multiplication sign).

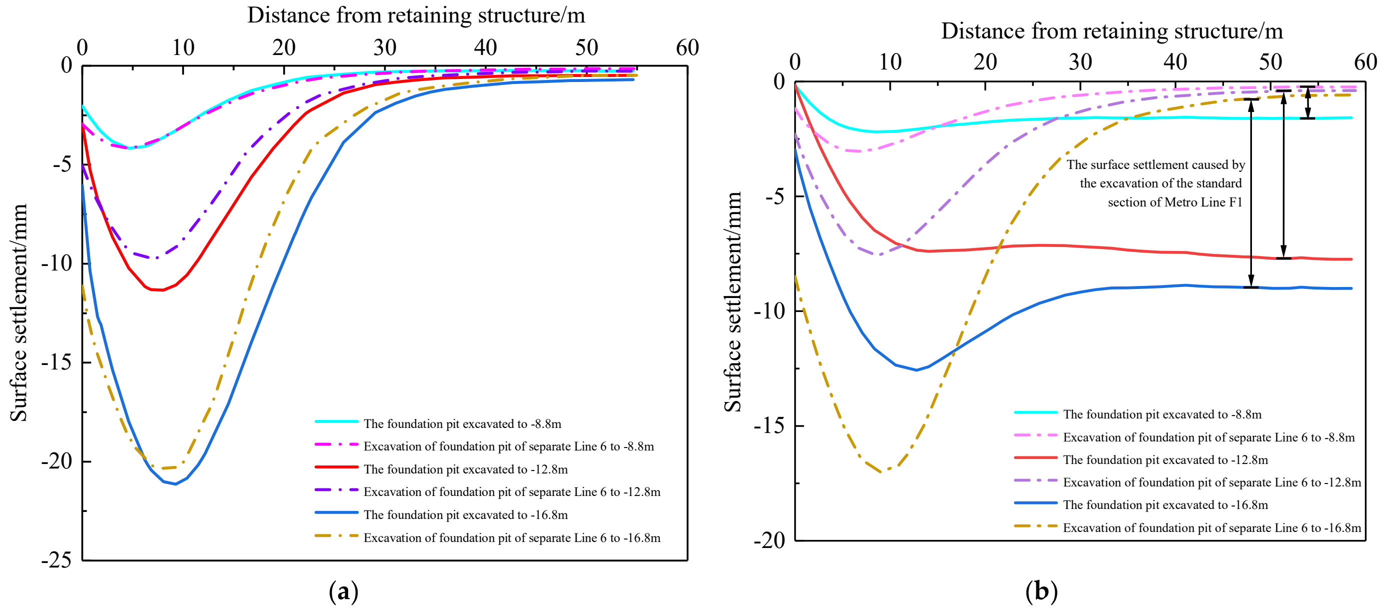

Figure 14. Surface settlement in a typical profile direction. (**a**) 1-1 profile direction; (**b**) 1-3 profile direction.

Figure 14a shows that the maximum surface settlement in Zone II (that is, the surface settlement along Profile 1-1) is 21.1 mm. When the foundation pit earthwork is excavated to the third layer, the maximum surface settlement changed greatly compared with the single excavation, and its value increased by 16.1%; however, after the excavation of the foundation pit, the maximum surface settlement only increased by 3.96%. The surface settlement in the direction of the 2-2 profile in Zone II also has similar deformation characteristics. It can be seen that when the adjacent foundation pits are excavated synchronously, the surface settlement in Zone II has a larger increase compared with the single excavation, while after the final excavation of the foundation pit, the maximum surface settlement increases slightly.

It can be seen from Figure 14b that the ground surface about 25 m away from the direction of Profile 1-3 has a large settlement deformation, which is roughly the same as the ground settlement of the standard section of Metro Line F1 excavated separately at the same location. At each stage of foundation pit excavation, the maximum surface settlement in the 1-3 profile direction is smaller than that caused by the separate excavation, and this reduction becomes gradually more obvious with the increase of the foundation pit excavation depth. After the final excavation, the maximum surface settlement decreases by 26%.

It can be seen that during the excavation of the traversing cross-type deep foundation pit, the deformation of the structure and soil in different areas at the cross position is influenced by different effects, thus forming different deformation characteristics compared with the excavation of the single foundation pit.

5. Influence of Disturbance and the Active Range of "Disturbance Influence Zone"

Through the above analysis, it can be seen that different deformation characteristics occur in the excavation process of cross-type deep foundation pits. The horizontal displacement and surface settlement of the retaining structure at the intersecting position are different compared with the excavation of individual foundation pits, indicating that there is a mutual influence on the deformation between foundation pits. In this study, the interaction between the structure and the soil at the intersection caused by the excavation of an additional foundation pit is collectively referred to as the "disturbance influence".

5.1. Influence of Excavation Disturbance on the Horizontal Displacement of the Retaining Structure

For the horizontal displacement of the foundation pit retaining structure, through the above analysis and research on the finite soil pressure [5], it was found that during the excavation of the foundation pit in this project, most of the soil at the intersection of Zone I is in a non-semi-infinite space state (i.e., the state of finite soil pressure). Due to the change in the soil boundary conditions [23], the soil arching effect [24], and unloading of adjacent foundation pits by multiple excavations, there is obvious interaction between the retaining structure and the surrounding soil mass. This reduces the earth pressure acting on the retaining structure (compared with the traditional earth pressure calculation) and weakens the lateral displacement of most of the retaining structures, with a reduction in the horizontal displacement compared with that of a single foundation pit excavation. For the 1-3 profile in Zone I, the maximum horizontal displacement decreases by 26.1%. This weakening effect on the horizontal displacement of the retaining structure is called the "disturbance positive influence", as shown in Figure 15.

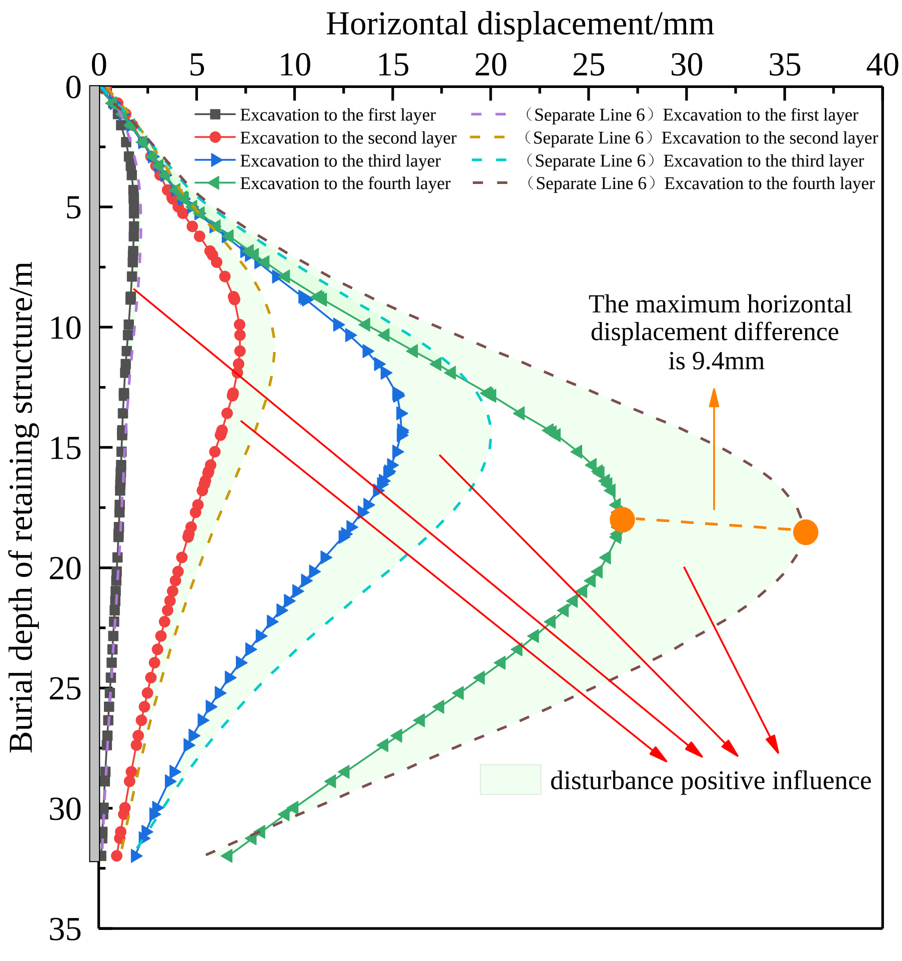

Figure 15. "Disturbance positive influence" of 1-3 profile of Zone I.

It can be seen from Figure 15 that when the foundation pit is excavated shallowly, the "disturbance positive influence" is very small. With an increase in the excavation depth, the weakening effect on the horizontal displacement of the retaining structure gradually becomes obvious.

In the retaining structure in Zone II, due to the repeated disturbance of excavation and unloading between the foundation pits, the lateral displacement of most of the retaining structures has an amplifying effect, so that the horizontal displacement increases compared with the excavation of individual foundation pits. For the 1-1 profile retaining structure of Metro Line 6, this disturbance effect is the most obvious; the maximum horizontal displacement increases by 20.4%. This effect of increasing the deformation of the retaining structure is called the "disturbance negative influence", as shown in Figure 16.

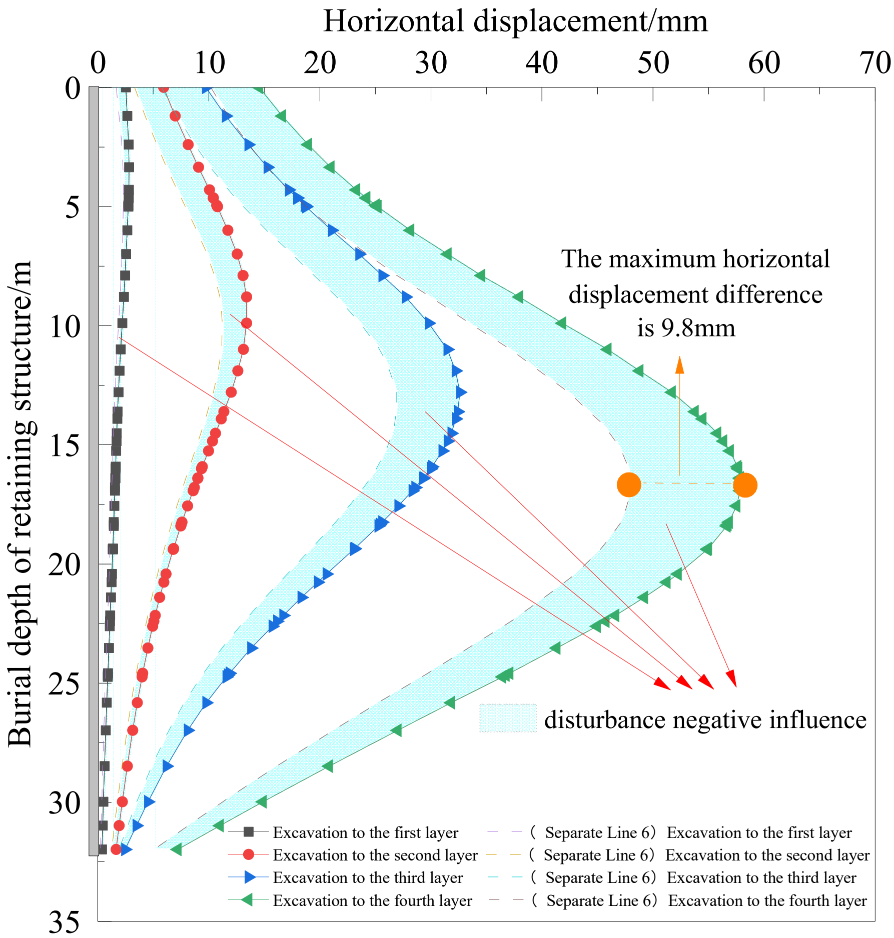

Figure 16. "Disturbance negative influence" of 1-1 profile of Zone II.

It can be seen from Figure 16 that the "disturbance negative influence" is also affected by the excavation depth of the foundation pit. With an increase in the excavation depth of the foundation pit, the amplification effect on the horizontal displacement of the retaining structure gradually becomes obvious. Therefore, it is necessary to consider how the depth of the foundation pit will influence the project when excavating the foundation pit.

5.2. Influence of Excavation Disturbance on Surface Settlement

It can be seen from Figure 14 that the disturbance caused by the excavation of a traversing cross-type deep foundation pit has a complex effect on the surface settlement; however, its effect on the maximum surface settlement is similar to the horizontal displacement of the retaining structure.

The maximum surface settlement of soil mass in Zone I is smaller than that seen in separate excavations. Figure 14b shows that the maximum surface settlement decreases at each stage, and the reduction effect becomes obvious as the excavation depth of the foundation pit increases.

As can be seen from Figure 14a, the maximum surface settlement of the soil in Zone II during the synchronous excavation of the foundation pit was greatly increased compared with a single excavation. However, when the fourth layer of the foundation pit of Metro Line 6 was finally excavated, the change in the maximum surface settlement was very small.

In the design and construction of this project, the horizontal displacement of the retaining structure will be prioritized. Empirically, the impact of excavation disturbance on the surface settlement is relatively complex; the following sections mainly focus on the retaining structure.

5.3. Research on the Active Range of the "Disturbance Influence Zone"

During the excavation of the cross-type deep foundation pit, the areas most easily disturbed at the intersection are termed the "disturbance influence zone". There is interaction between the structure and the soil in this area; the ability to determine its active range is of great significance for the safety, stability, and economy of the project.

To explore the range of mutual influence of adjacent foundation pit excavations, Zhang et al. [25] believe that the critical distance, where there is no mutual influence of adjacent parallel foundation pits under synchronous construction, is about 1.7 H (H represents the depth of foundation pit). Xiaoyu Chen [7] believes that the distance of deformation without mutual influence is 3.0 H. However, the adjacent foundation pit in this project is of an intersection type and the depth of the foundation pit is also different, with a certain degree of spatial effects on the disturbance [26–28]. Through an analysis of the deformation characteristics, at the position 3.0 times the pit depth from the retaining structure, the horizontal displacement of the retaining structure of the deeper foundation pit is still quite different from that of the individual excavation. Therefore, the effect of disturbance still plays a significant role in the deformation of the foundation pit, and it is thus necessary to reconsider the active range of the "disturbance influence zone" of the project (Zone I and Zone II).

Assuming that the distance between the retaining structure profile and the intersection of the two foundation pits is d (d is the distance from the intersection of the foundation pits to the selected structure profile, as shown in Figure 9), the deformation characteristics of the retaining structure are analyzed at different locations (separate foundation pits and adjacent foundation pits). The retaining structure profile is selected as the critical location without disturbance when the change in the maximum horizontal displacement difference remains unchanged [7,25]. At this time, the influence of disturbance caused by adjacent foundation pit excavations on the horizontal displacement of the retaining structure can be ignored.

For the foundation pit of Metro Line 6, the part located in Zone I, when d = 3.5 He (He is the depth of the foundation pit of Metro Line 6) from the intersection, the maximum horizontal displacement difference of its retaining structure is 0.071 mm, which is 0.15% of the excavation of the foundation pit of Line 6 alone. The disturbance effect caused by the excavation can be ignored, as shown in Figure 17. Beyond this distance, the horizontal displacement of the retaining structure is similar to that under the single excavation condition. The results of the analysis show that the active range of the "disturbance influence zone" is 3.5 times the depth of the foundation pit (deeper foundation pit) of Metro Line 6.

However, for the part of Metro Line 6 located in Zone II, the horizontal displacement of most of its retaining structures is greater than for the excavation of a single foundation pit. For this project, the impact of disturbance on the retaining structures located in this area is considered to be a "disturbance negative influence", which is more conducive to the safety of the foundation pit.

For the foundation pit of the standard section of Metro Line F1, when d = 3.0 He from the intersection, the difference in the maximum horizontal displacement of the retaining structure in Zone I is 0.32% of that seen for the excavation of a single foundation pit. For the retaining structure in Zone II, the difference in its maximum horizontal displacement is 0.51% of the displacement of a single foundation pit, as shown in Figure 18a,b. Beyond this distance, the disturbance effect can be ignored. The analysis results show that the active range of the "disturbance influence zone" is 3.0 times that of the deeper foundation pit.

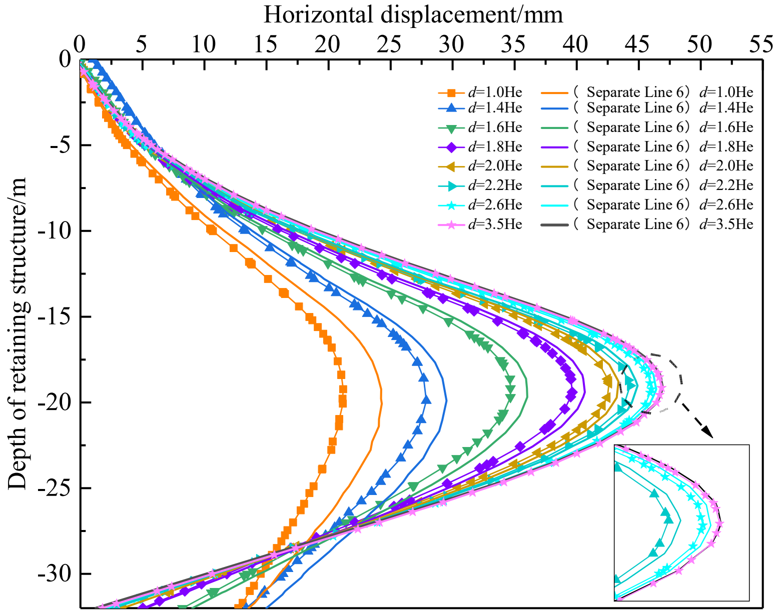

Figure 17. Horizontal displacement of the retaining structure in the direction of Metro Line 6 (Zone I).

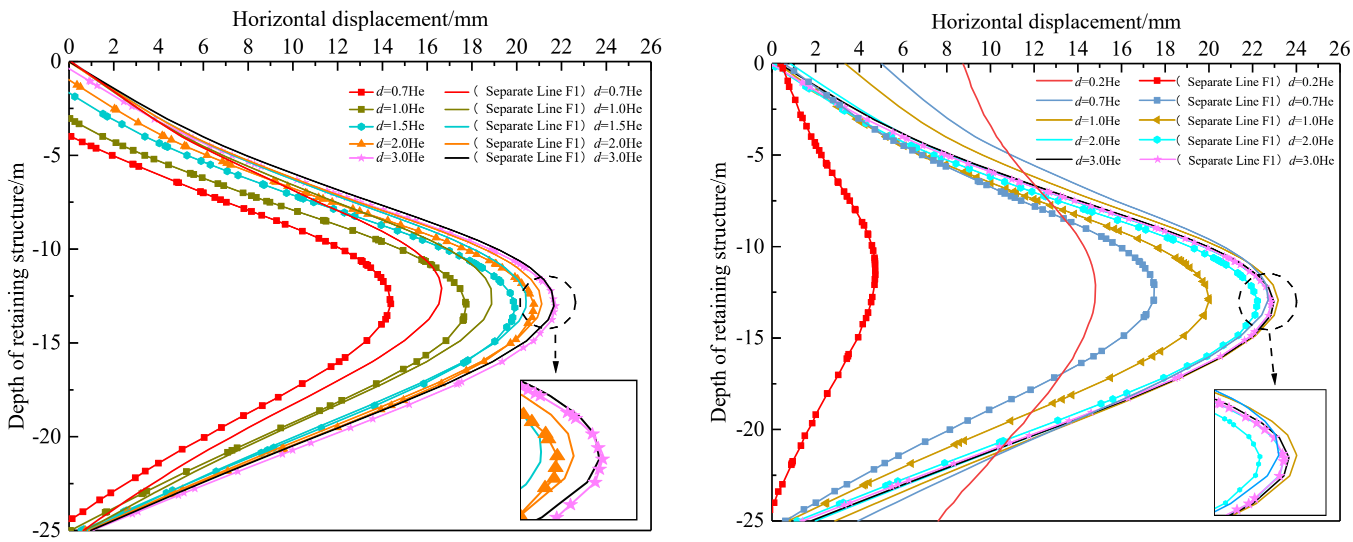

Figure 18. Horizontal displacement of the retaining structure in the direction of Metro Line F1. (**a**) Zone I; (**b**) Zone II.

When studying the active range of the "disturbance influence zone", it can be clearly seen that most of the retaining structures of the foundation pit located in Zone I are under the action of the "disturbance positive influence". However, most of the retaining structures of the foundation pit located in Zone II are under the action of the "disturbance negative influence". Before commencing construction of this project, a reasonable structural arrangement for the foundation pit within the active range of the "disturbance affected zone" can effectively ensure the smooth progress of the project.

6. Discussion

6.1. Main Factors Affecting the Active Range of the "Disturbance Influence Zone"

According to the survey report and considering that the project is located in a coastal area, the groundwater level may fluctuate greatly during the excavation of the foundation pit, and the time required for the construction of the foundation pit project considerable. Therefore, changes in the groundwater level are an extremely important consideration for the project.

6.2. Change in Groundwater Level

Because changes in the groundwater level are an unknown during the construction process, it is difficult to dynamically adjust the groundwater level in the numerical simulations. To facilitate the calculation, different static groundwater level changes were used to simulate the changes in the groundwater level. According to the recent on-site groundwater level survey results, simulated groundwater level depths of −1.5 m, −1.75 m, −2.0 m, −2.25 m, −2.75 m, −3.0 m, −3.25 m, and−3.5 m were selected for comparison with the active range of the "disturbance influence zone" when the groundwater depth is −2.5 m.

It can be seen from Figure 19 that the active range of the "disturbance influence zone" for the horizontal displacement of the retaining structure increases with a decrease in the groundwater depth, which has an obvious impact on the deeper foundation pit. For the deformation of the retaining structure, the drawdown of the groundwater level reduces the deformation of the structure to a certain extent, which is beneficial to the project. When the groundwater level is shallow, the groundwater needs to be treated accordingly to ensure the smooth excavation of the foundation pit.

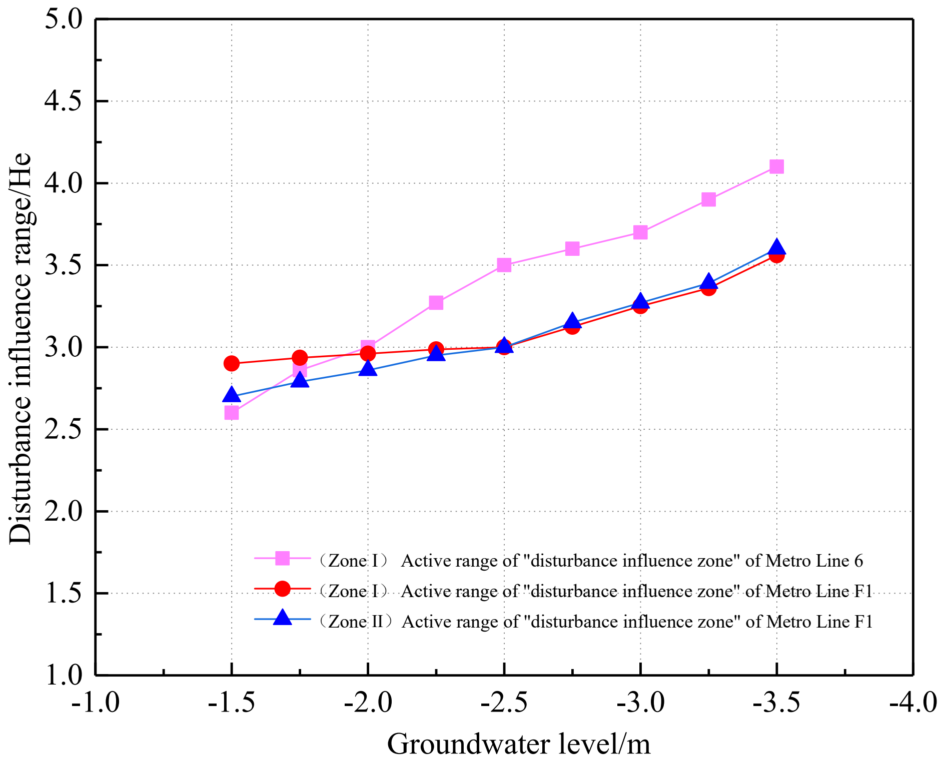

Figure 19. The relationship between the depth of groundwater level and the active range of the "disturbance influence zone".

The influence of a change in the groundwater level on the active range of the "disturbance influence zone" should be considered in the project construction. In the excavation stage of the foundation pit, the groundwater level is monitored in real-time and assessed comprehensively to obtain a more accurate active range of the “disturbance influence zone”, in order to reasonably adjust and control the structure.

7. Conclusions

Based on the finite element simulation of the foundation pit of Fuzhou Coastal New City, the deformation characteristics, disturbance effects, and active range of the excavation of the traversing cross-type deep foundation pit are studied. The main conclusions are as follows:

(1) According to the different effects to the structure and soil affected by excavation disturbances in different areas of the intersection, the positive and negative effects of the disturbances are divided. The retaining structure in Zone I is mainly affected by a “disturbance positive influence”, such as profile 1-3, whose maximum horizontal displacement is reduced by 26.1% compared to that of the single foundation pit excavation, while the retaining structure in Zone II is mainly affected by a “disturbance negative influence”, such as profile 1-1, whose maximum horizontal displacement is increased by 20.4% compared to that of the single foundation pit excavation. This disturbance effect gradually becomes apparent with an increase in the excavation depth of the foundation pit, and there is a certain range of action.

(2) For the foundation pit of Metro Line 6, the active range of the “disturbance influence zone” of the horizontal displacement of the retaining structure of the part located in Zone I is 3.5 times that of the deeper foundation pit. At this critical position, compared with the single foundation pit, the difference in maximum horizontal displacement is 0.15% of that of the individual excavation. The section in Zone II is within the active range of the “disturbance influence zone”. For the foundation pit of Metro Line F1, the active range of the “disturbance influence zone” of the horizontal displacement of the retaining structure in Zone I and Zone II is 3.0 times that of the deeper foundation pit. At this critical position, the difference in the maximum horizontal displacement is 0.32% and 0.51% respectively.

(3) The active range of the “disturbance influence zone” of the horizontal displacement of the retaining structure shows an increasing trend with the decline of the groundwater level, and there is a more obvious impact on the deeper foundation pit.

Author Contributions: Conceptualization and methodology, S.W.; software, B.Y.; validation, Z.Z.; formal analysis, S.W.; investigation, F.D.; writing—original draft preparation, B.Y.; writing—review and editing, B.Y. and M.M.; supervision, project administration and funding acquisition, S.W. All authors have read and agreed to the published version of the manuscript.

Funding: The authors gratefully acknowledge the financial support from the National Natural Science Foundation of China (Grant No. U1602232), the Liaoning Province Science and technology plan, China (2019JH2-10100035), the Fundamental Research Funds for the Central Universities (N170108029, Grant No. 2101018).

Institutional Review Board Statement: Not applicable.

Informed Consent Statement: Not applicable.

Data Availability Statement: Not applicable.

Acknowledgments: The authors would like to thank the reviewers for their many constructive suggestions and comments that helped improve the quality of the paper.

Conflicts of Interest: The authors declare no conflict of interest.

Abbreviations

c'	effective cohesion
φ'	effective friction angle
E_{oed}^{ref}	oedometric loading modulus

E_{50}^{ref}	triaxial loading Young's modulus when shear stress is 50% of shear strength
E_{ur}^{ref}	unloading–reloading Young's modulus
G_0^{ref}	reference shear stiffness
$\gamma_{0.7}$	a reference shear strain at which shear stiffness is 70% of G_0^{ref}
m	the power parameter for stress-dependency of stiffness
K_0	static lateral pressure coefficient of normal consolidation
R_f	damage ratio

References

1. Wang, Y.; Gao, D.; Meng, C. Numerical Simulation Analysis on the Lateral Dynamic Characteristics of Deepwater Conductor Considering the Pile-Soil Contact Models. *J. Mar. Sci. Eng.* **2022**, *10*, 1540. [CrossRef]
2. Lin, Z.; Xie, S.; Xia, C.; Dou, H. Design and Practice of Deep Foundation Pits for Large Storage Ponds in Complex Environments. *Sustainability* **2022**, *14*, 14046. [CrossRef]
3. Feng, X.; Hou, D.; Huang, Z. The Influence of Shield Tunneling Characteristics on the Safety of Buildings Above-Case Study for Shanghai Zone. *Sustainability* **2022**, *14*, 13391. [CrossRef]
4. Yang, T.; Xiong, S.; Liu, S.; Liu, Y.; Zhao, H. Numerical analysis of the influence of deep foundation pit construction on adjacent subway stations in soft soil areas. *Adv. Civ. Eng.* **2022**, *2022*, 6071868. [CrossRef]
5. Talebinejad, A.; Chakeri, H.; Moosavi, M.; Ozcelik, Y.; Unver, B.; Hindistan, M.A. Investigation of surface and subsurface displacements due to multiple tunnels excavation in urban area. *Arab. J. Geosci.* **2014**, *7*, 3913–3923. [CrossRef]
6. Lai, F.W.; Liu, S.Y.; Yang, D.Y.; Cheng, Y.H.; Fan, Q.J. Generalized solution to active earth pressure exerted onto retaining wall with narrow backfills. *Chin. J. Geotech. Eng.* **2022**, *44*, 483–491.
7. Chen, X.Y.; Yuan, J.; Hu, M.Y.; Zhang, Y. Theoretical analysis and numerical simulation of safe distance of adjacent deep foundation pits. *Chin. J. Undergr. Space Eng.* **2019**, *15*, 1557–1564+1572.
8. Song, D.; Chen, Z.; Dong, L.; Tang, G.; Zhang, K. Monitoring analysis of influence of extra-large complex deep foundation pit on adjacent environment: A case study of Zhengzhou City, China. *Geomat. Nat. Hazards Risk* **2020**, *11*, 2036–2057. [CrossRef]
9. Zeng, F.Y.; Zhang, Z.J.; Wang, J.H.; Li, M.G. Observed performance of two adjacent and concurrently excavated deep foundation pits in soft clay. *J. Perform. Constr. Facil.* **2018**, *32*, 04018040. [CrossRef]
10. Chen, S.; Cui, J.; Liang, F. Case Study on the Deformation Coupling Effect of a Deep Foundation Pit Group in a Coastal Soft Soil Area. *Appl. Sci.* **2022**, *12*, 6205. [CrossRef]
11. Li, L.X.; Liu, J.D.; Zhang, Q.; Qiu, H.; Jia, B. Three-dimensional finite element analysis and deformation control of excavation with common-wall of parallel metro stations. *J. Railw. Eng. Soc.* **2021**, *38*, 13–18+30.
12. Hou, Y.M.; Wang, J.H.; Zhang, L.L. Finite-element modeling of a complex deep excavation in Shanghai. *Acta Geotech.* **2009**, *4*, 7–16. [CrossRef]
13. Ardakani, A.; Bayat, M.; Javanmard, M. Numerical modeling of soil nail walls considering Mohr Coulomb, hardening soil and hardening soil with small-strain stiffness effect models. *Geomech. Eng.* **2014**, *6*, 391–401. [CrossRef]
14. Kawa, M.; Puła, W.; Truty, A. Probabilistic analysis of the diaphragm wall using the hardening soil-small (HSs) model. *Eng. Struct.* **2021**, *232*, 111869. [CrossRef]
15. Castellón, J.; Ledesma, A. Small strains in soil constitutive modeling. *Arch. Comput. Methods Eng.* **2022**, *29*, 3223–3280. [CrossRef]
16. Luo, M.M.; Chen, Y.; Zhou, J. Research status and prospect of parameter selection for the HS-SMALL model. *Ind. Constr.* **2021**, *51*, 172–180. [CrossRef]
17. Wang, S.; Jierula, A.; Wang, P.; Zhao, Y. Mechanical behaviors of "easy cracking zones" of precast rectangular utility tunnels. *Case Stud. Constr. Mater.* **2021**, *15*, e00648. [CrossRef]
18. Huang, M.; Liu, X.R.; Zhang, N.Y.; Shen, Q.W. Calculation of foundation pit deformation caused by deep excavation considering influence of loading and unloading. *J. Cent. South Univ.* **2017**, *24*, 2164–2171. [CrossRef]
19. Sun, Y.; Xiao, H. Wall displacement and ground-surface settlement caused by pit-in-pit foundation pit in soft clays. *KSCE J. Civ. Eng.* **2021**, *25*, 1262–1275. [CrossRef]
20. Niu, J.D.; Li, Z.W.; Xiao, J.; Wang, K.H. Deformation calculation and supporting performance of foundation pit considering stress path. *J. Railw. Sci. Eng.* **2021**, *18*, 71–80.
21. Hsieh, P.G.; Ou, C.Y. Shape of ground surface settlement profiles caused by excavation. *Can. Geotech. J.* **1998**, *35*, 1004–1017. [CrossRef]
22. Yang, J.; Kong, D. Deformation of deep and large foundation pit in soft soil of Fuzhou Subway. *Arab. J. Geosci.* **2020**, *13*, 36. [CrossRef]
23. Huang, K.; Liu, R.; Sun, Y.; Li, L.; Xie, Y. Study on the calculation method of active earth pressure and critical width for finite soil behind the retaining wall. *Front. Earth Sci.* **2022**, *10*, 883668. [CrossRef]
24. Karl, T. *Theoretical Soil Mechanics*; John Wiley & Sons, Inc.: Hoboken, NJ, USA, 1943.
25. Zhang, Z.J.; Li, M.G.; Chen, J.J.; Wang, J.H.; Zeng, F.Y. Innovative construction method for oversized excavations with bipartition walls. *J. Constr. Eng. Manag.* **2017**, *143*, 04017056. [CrossRef]

26. Zhang, L.; Hao, Z.; Chai, S.; Zhou, Y. Unloading mechanical effect analysis of retaining structure of deep foundation pit in soft soil. *IOP Conf. Ser. Earth Environ. Sci.* **2019**, *252*, 052054. [CrossRef]
27. Finno, R.J.; Blackburn, J.T.; Roboski, J.F. Three-dimensional effects for supported excavations in clay. *J. Geotech. Geoenvironmental Eng.* **2007**, *133*, 30–36. [CrossRef]
28. Yang, T.; Liu, S.L.; Wang, X.Y.; Zhao, H.; Liu, Y. Analysis of the deformation law of deep and large foundation pits in soft soil areas. *Front. Earth Sci.* **2022**, *10*, 828354. [CrossRef]